DOI 10.1590/s1982-21702022000100003

ORIGINAL ARTICLE

Orthometric, normal and geoid heights in the context of the Brazilian altimetric network

Danilo Fernandes de Medeiros[1] - ORCID: 0000-0002-9710-7001
Giuliano Sant'Anna Marotta[1] - ORCID: 0000-0003-1073-0683
Carlos Alberto Moreno Chaves[2] - ORCID: 0000-0001-6414-3295
George Sand Leão Araújo de França[1] - ORCID: 0000-0002-2694-5868

[1] Universidade de Brasília, instituto de Geociências, Brasília – Distrito Federal, Brasil.
E-mail: danilofmedeiros@yahoo.com.br; marota@unb.br, georgesand@unb.br

[2] Universidade de São Paulo, Instituto de Astronomia, Geofísica e Ciências Atmosféricas, São Paulo – São Paulo, Brasil.
E-mail: carlos.chaves@iag.usp.br

Received on 25th March 2021.
Accepted on 02nd February 2022.

Abstract:

The extensive use of GNSS positioning, combined with the importance of precise geoid heights for transformation between geodetic and orthometric heights, brings up the discussion of the influence of data uncertainties and the use of variable density values on these estimates. In this sense, we analyze the influence of the topographic masses density distribution and the data uncertainty on the computation of orthometric and geoid heights in stations of the High Precision Altimetric Network of Brazil, considering the Helmert and Mader methods. For this, we use 569 stations whose values of geodetic and normal heights, gravity, and geopotential numbers are known. The results indicate that orthometric heights are more sensitive to density values and to greater heights than to the Helmert and Mader methods applied. Also, we verify that the normal and orthometric heights present significant differences for the analyzed stations, considering the high correlation between the heights, which provide small values of uncertainty. However, our analyses show that the use of the Mader method, along with variable density values, provides either more rigorous or more reliable results.

Keywords: Density; Geoid; Normal Heights; Orthometric Heights; Uncertainty.

How to cite this article: MEDEIROS, D.F.; MAROTTA, G.S.; CHAVES, C.A.M.; FRANÇA, G.S.L.A. Orthometric, normal and geoid heights in the context of the brazilian altimetric network. *Bulletin of Geodetic Sciences*. 28(1): e2022003, 2022.

1. Introduction

Engineering works, hydrodynamic and hydrological studies are elements positioned in space that require appropriate geodetic references. However, despite the precise geodetic system being now available, the vertical system does not have a consolidated regional or global reference. According to Sánchez and Freitas (2016), for example, the South American countries currently do not have a single vertical reference system and, therefore, each country has its own vertical datum associated with a level surface obtained from one or more tide gauges records.

Aiming at the unification of the altimetric system, the Geocentric Reference System for the Americas (SIRGAS) following the resolution No. 1/2015 of the International Association of Geodesy (IAG 2015), which discusses the International Height Reference System (IHRS), has been working to define a Vertical Reference Frame for the Americas as well as heights, normal or orthometric, despite the recommendation for the use of normal heights.

Due to the range of choices, different countries have been adopting different heights, such as orthometric, in Argentina (IGN 2017), and normal, in Brazil, where its use is based on geopotential numbers (IBGE 2018).

Regarding the choice of which height is more appropriate to use, there are still many discussions in the scientific community. On the one hand, it is important to use the geoid and orthometric heights. On the other hand, because of the impossibility of knowing the density distribution of the topographic masses with good accuracy, it is prudent to use a conventional surface that approaches the geoid (the quasi-geoid) and the normal heights.

Due to the exposed problems, many studies (Tenzer et al. 2006; Flury and Rummel 2009; Ferreira et al. 2011; Albarici et al. 2018; Sjöberg 2018; Tocho et al. 2020) have been working on improving the computation of the geoid-quasigeoid separation and, consequently, in a way to relate orthometric and normal heights. Along with these studies, the use of more detailed topographic masses lateral density models has provided better accuracy in the computation of orthometric heights and, consequently, in a more rigorous computation of the geoid-quasigeoid separation (Pick et al. 1973; Vaníček et al. 2003).

Given the above, in this study, we analyze the influence of the topographic masses density distribution and the data uncertainty on the computation of orthometric and geoid heights in stations of the High Precision Altimetric Network (RAAP), using both Helmert's method (Helmert 1890) and Mader's method (Mader 1954). These stations are part of the Brazilian Geodetic System (SGB) and are maintained by the Brazilian Institute of Geography and Statistics (IBGE).

2. Normal, Orthometric and Geoid Heights

According to Torge (1991), the geopotential number (C) is the preferable quantity for describing the behavior of the masses in the gravitational field. However, C does not meet the demand for a height system that works on the metric unit. In this case, the height (H_F) can be described by the following expression (Heiskanen and Moritz 1967; Torge 1991):

$$C = W_0 - W_P = -\int_0^P dW = \int_0^P g\, dH \cong \sum_{i=1}^{n} \bar{g}_i \, \Delta H_i \tag{1}$$

$$H_F = \frac{C}{g'} \tag{2}$$

W_0 and W_P are the gravity potentials at the geoid and point (P) level, respectively; g and $\bar{g}$ represent the terrestrial and the mean gravity values observed on the surface, respectively; ΔH is the height difference; and g' is a particular value of gravity.

Drewes et al. (2002) showed that the height type, the reference surface, the realization and maintenance of the reference system are the main topics to define the vertical reference system, for SIRGAS, and recommended the introduction of two height types, geodetic or ellipsoidal (h) and normal (H_N). In this context, H_N is defined considering the mean value of normal gravity ($\bar{\gamma}$) (Equation 3; Figure 1). According to Heiskanen and Moritz (1967), we have:

$$H_N = \frac{C}{\bar{\gamma}} \tag{3}$$

$$\bar{\gamma} = \gamma_0 \cdot \left[1 - \frac{H_N}{a}\left(1 + f + m - 2 f \sin^2\varphi\right) + \left(\frac{H_N}{a}\right)^2 \right] \tag{4}$$

$$\gamma_0 = \gamma_a \frac{1 + k \sin^2\varphi}{\sqrt{1 - e^2 \sin^2\varphi}} \tag{5}$$

$$k = \frac{b\gamma_b - a\gamma_a}{a\gamma_a} \tag{6}$$

$$m = \frac{\omega^2 a^2 b}{GM} \tag{7}$$

φ represents the geodetic latitude; a, b, e, and f represent the major and minor axes, the first eccentricity and the flattening of the reference ellipsoid, respectively; γ_a, γ_b and γ_0 represent normal gravity, at the equator, the pole and the considered point, respectively; and ω and GM represent the angular velocity and the geocentric gravitational constant. All presented parameters are associated with the adopted reference ellipsoid.

Using the geoid as a reference in Equation (2), we have the orthometric height (H) as a definition, and the mean value of gravity ($\bar{g}$) measured along the plumb line (Equation 8, Figure 1). Thus, we need to know the values of gravity inside the Earth. Nevertheless, this is not yet possible because of the difficulty of estimating the density distribution inside the Earth with good accuracy (e.g., Marotta 2020).

$$H = \frac{C}{\bar{g}} \tag{8}$$

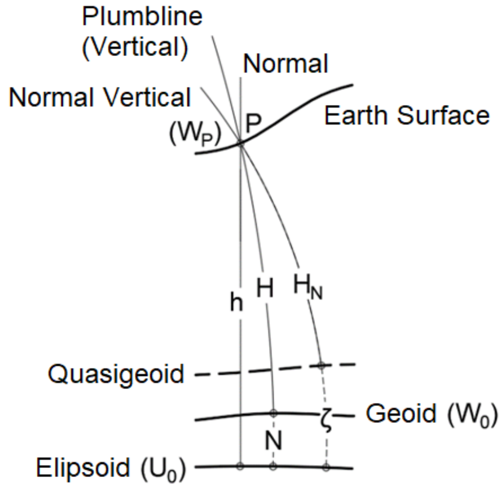

Figure 1: Ellipsoidal (h), orthometric (H) and normal (H_N) heights, together with geoid height (N) and height anomaly (ζ) at the P point. U_0 represents the normal potential, and W_0 and W_p the gravity potentials at the geoid and P point level, respectively. Adapted from Torge (1991), IBGE (2018) and Marotta (2020).

Despite the difficulty to compute H values for the explained reasons and considering the importance of using the geoid as a reference, some approaches have been developed (Helmert 1890; Niethammer 1932; Ramsayer 1953 and 1954; and Mader 1954), which are based on assumptions for computing the mean value of gravity along the plumb line. Among the different assumptions, those developed by Helmert (1890) and Mader (1954) have been widely used.

Helmert's orthometric height (H_H) assumes that gravity varies linearly with height. In this case, the simplified Poincaré-Prey reductions (Heiskanen and Moritz 1967; Torge 1991) are applied to estimate the mean value of gravity ($\bar{g}_H$) along the plumb line as follows:

$$\bar{g}_H = g - \frac{1}{2}\frac{\partial g}{\partial H}H - 2\pi G\rho H \tag{9}$$

where $\frac{\partial g}{\partial H}H$ can be estimated as suggested by Featherstone and Dentith (1997):

$$\frac{\partial g}{\partial H}H \approx \frac{2\gamma_0}{a}H\left[1+f+m-2f\,sin^2\varphi\right]-\frac{3\gamma_0 H^2}{a^2} \tag{10}$$

Here, g is the observed gravity at the point of interest; G is the universal gravitational constant; ρ is the density; H is the orthometric height; φ is the geodetic latitude; a and f represent the major axis and the flattening of the reference ellipsoid, respectively; m is computed using equation (7); and γ_0 represents the normal gravity at the considered point. It is worth mentioning that the Poincaré-Prey reduction applies simplifications with respect to mass distribution of topography above the geoid and neglects the roughness of the residual terrain (Santos et al. 2006).

Mader's orthometric height (H_M) includes in H_H the terrain corrections (Mader 1954; Heiskanen and Moritz 1967; Dennis and Featherstone 2003), computed on the topographic surface (C_{Tp}) and geoid (C_{Tg}), to provide a more realistic mean value of gravity ($\bar{g}_M$):

$$\bar{g}_M = g - \frac{1}{2}\frac{\partial g}{\partial h}H - 2\pi G\rho H + \frac{\left(C_{Tp}-C_{Tg}\right)}{2} \tag{11}$$

where C_{Tp} and C_{Tg} can be computed as demonstrated by Hwang and Hsiao (2003):

$$C_{Tp} = G\iint_E \int_{z=H_p}^{H} \frac{\rho(x,y,z)(z-H_p)}{\left[\sqrt{(x-x_p)^2+(y-y_p)^2+(z-H_p)^2}\right]^3} dxdydz \tag{12}$$

$$C_{Tg} = G\iint_E \int_{z=H_p}^{H} \frac{\rho(x,y,z)z}{\left[\sqrt{(x-x_p)^2+(y-y_p)^2+z^2}\right]^3} dxdydz \tag{13}$$

Here, E is the integration area, ρ is the density at the integration point, x and y are the planimetric coordinates, and z and H_p are the orthometric heights of the integration and computation points (P), respectively. Flury and Rummel (2009) highlighted that albeit $\overline{g}_M$ incorporates a rigorous approach to the topographic attraction at both extremities of the plumb line, on the surface and geoid, non-linear changes between them are neglected.

Once the values of h, H and H_N are known and considering the height anomaly (ζ), the geoid height (N) can be computed using an algebraic relationship (Equations 14 and 15) as presented by Heiskanen and Moritz (1967) and Sjöberg (2010) as follows:

$$N \cong h - H \tag{14}$$

$$\zeta \cong h - H_N \tag{15}$$

$$\zeta - N \cong \Delta HH_N = H - H_N \tag{16}$$

Within the presented relations for computing H and N, the density, ρ, as a physical property that influences the variation of the Earth's gravity field, is directly related to the achieved result. According to Flury and Rummel (2009) and Hinze (2003), for topographic masses, ρ can vary between 10 to 20% from the mean density value of 2670 kg/m³, which is historically adopted by several works, since it is influenced by depth, mineralogical composition and geological events that affect the stratification of rock layers within the Earth.

Despite the difficulty of estimating three-dimensional models, many studies have been trying to estimate and use more reliable models of topographic masses lateral density (Martinec et al. 1995; Pagiatakis and Armenakis 1999; Kuhn 2000; Huang et al. 2001; Tziavos and Featherstone 2001; Rózsa 2002; Sjöberg 2004; Kiamehr 2006; Tenzer et al. 2011; Marotta et al. 2019; Sheng et al. 2019). These global, regional or local models have been developed mainly through geological maps combined with rocks density values or their arrangements, collected in the field.

From the presented formulations, the data and its uncertainty, for the computation procedure, we can also estimate and analyze the uncertainties (σ), using the general law of variance propagation. Consequently, once the values and uncertainties of HN, g and ρ are known, and excluding other sources of uncertainties, we can evaluate their influence on the computation of H, N, and on the differences between H and H_N, here called ΔHH_N, as follows:

$$\sigma_H = \sqrt{\left(\frac{\partial H}{\partial H_N}\right)^2 \sigma_{H_N}^2 + \left(\frac{\partial H}{\partial g}\right)^2 \sigma_g^2 + \left(\frac{\partial H}{\partial \rho}\right)^2 \sigma_\rho^2} \tag{17}$$

$$\sigma_{\Delta HH_N} = \sqrt{\left(\frac{\partial \Delta HH_N}{\partial H}\right)^2 \sigma_H^2 + \left(\frac{\partial \Delta HH_N}{\partial H_N}\right)^2 \sigma_{H_N}^2 - 2\sigma_{H,H_N}^2 \left(\frac{\partial \Delta HH_N}{\partial H}\frac{\partial \Delta HH_N}{\partial H_N}\right)} \tag{18}$$

$$\sigma_N = \sqrt{\left(\frac{\partial N}{\partial H}\right)^2 \sigma_H^2 + \left(\frac{\partial N}{\partial h}\right)^2 \sigma_h^2} \tag{19}$$

To estimate σ_H, $\sigma_{\Delta HH_N}$ and σ_N, we use Equations (16) and (14) along with a new one, which is obtained by combining Equations (3) and (8):

$$H = \frac{\bar{\gamma} H_N}{\bar{g}} \tag{20}$$

where H and $\bar{g}$ assume the complete formulations presented for the Helmert and Mader methods. The term σ^2_{H,H_N} from Equation (18) is calculated using the following equation:

$$\sigma^2_{H,H_N} = \left(\frac{\partial H}{\partial H_N} \right)^2 \sigma^2_{H_N} \tag{21}$$

3. *H, ΔHH$_N$* and *N* in the context of the Brazilian High Precision Altimetric Network (RAAP)

Since 2018 and according to recommendations presented by Drewes et al. (2002), Brazil has adopted H_N and C (IBGE 2018) to define the RAAP. However, it is considered that H and ΔHH_N are very important not only to establish the relationships between the different types of height but also to support the development of other models, such as the geoid models. Thus, this study includes the use of RAAP data, which is provided by IBGE; two models of lateral density of topographic masses (30 arc-seconds grid spacing), the LTD_Brazil, from Medeiros et al. (2021), and the UNB_TopoDensT, from Sheng et al. (2019); and the Digital Elevation Model (DEM), from the Shuttle Radar Topography Mission – SRTM, with 3 arc-second grid spacing (Farr et al. 2007).

We use 569 stations from the RAAP, with known values of $h \pm \sigma_h$, $H_N \pm \sigma_{H_N}$, C and g (Figure 2). To compute $\bar{g}$ for each station, $H \pm \sigma_H$ and $\Delta HH_N \pm \sigma_{\Delta HH_N}$ are estimated considering constant and variable (LTD_ Brazil and UNB_TopoDensT models) values of $\rho \pm \sigma_\rho$ and the Helmert and Mader methods. Also, to compute $C_{Tp} \pm \sigma_{Tp}$ and $C_{Tg} \pm \sigma_{Tg}$ (using topographic mass line model according to Li and Sideris 1994), which are part of the Mader method, integration radius up to 167 km, corresponding to ~1.5° or 166.7 km of the Hayford-Bowie zone (Hayford and Bowie 1912), and height data, from the DEM, are used. We assume the value of 0.01 mGal as uncertainty for g at all stations, considering the resolution of the most used gravimeter type in Brazil and Latin America (Amarante and Trabanco 2016), the Lacoste & Romberg model G gravimeter.

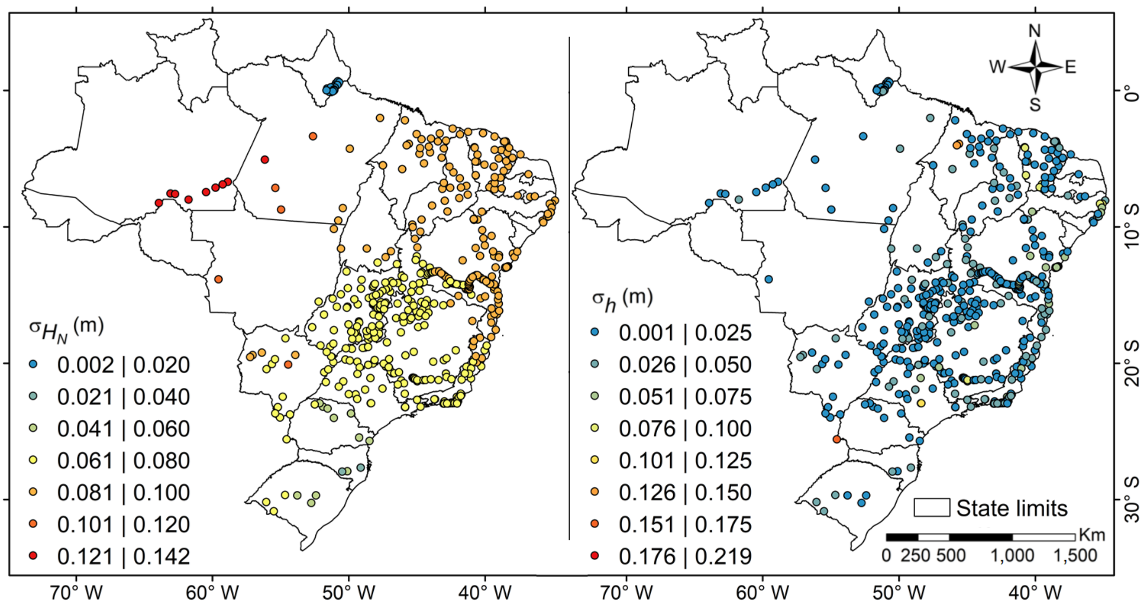

Figure 2: RAAP stations and distribution of the σ_{H_N} and σ_h values associated with the H_N and h values used in this study.

Following Hinze (2003) and Sheng et al. (2019), for $\rho \pm \sigma_\rho$ constant, we use the average value of 2670±800 kg/m³. For $\rho \pm \sigma_\rho$ variable, we use values from the LTD_Brazil model when we are inside the study area (Brazil), and density values from the UNB_TopoDensT model for regions outside (Figure 3). In addition, for the oceanic region, we assume H = 0 m for the mean sea level and a seawater density value of 1030±0 kg/m³ (García-Abdeslem 2020).

We use the LTD_Brazil model in the study area instead of the UNB_TopoDensT model because of its more detailed characteristic since it was developed using the Geological Map of Brazil (Bizzi et al. 2003), with a scale of 1:2,500,000, in which 78 types of generalized rock, from the 369 types originally identified, were used. The UNB_TopoDensT model was derived considering 15 main lithological units extracted from the Global Lithosphere Model (GLiM).

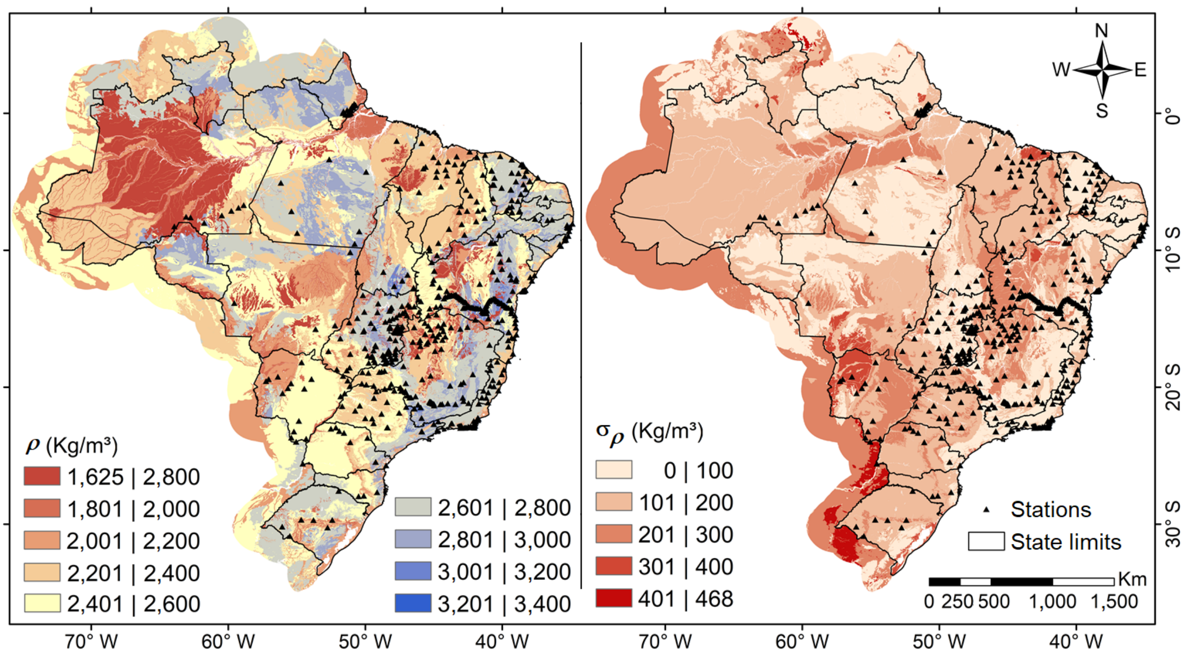

Figure 3: Selected RAAP stations (in black) on the topographic masses lateral density maps (left panel map) and the density uncertainties maps (right panel map) from the LTD_Brazil (Brazil) and UNB_TopoDensT (outside Brazil) models.

After computing $H \pm \sigma_H$ and $\Delta HH_N \pm \sigma_{\Delta HH_N}$ for the RAAP stations, we analyze the sensitivity of the results in relation to the used ($H_N \pm \sigma_{H_N}$) and estimated ($H_H \pm \sigma_{H_H}$ and $H_M \pm \sigma_{H_M}$) data to identify the presence of significant differences among all the values. After this analysis, $N \pm \sigma_N$ are computed for all stations used in this work.

4. Results and Discussions

To compare the difference between the estimated values of H and σ_H, using Helmert and Mader methods, for both constant and variable density values, in Figure 4 we analyze the estimated values of ΔHH_N and $\sigma_{\Delta HH_N}$ from the Helmert and Mader methods.

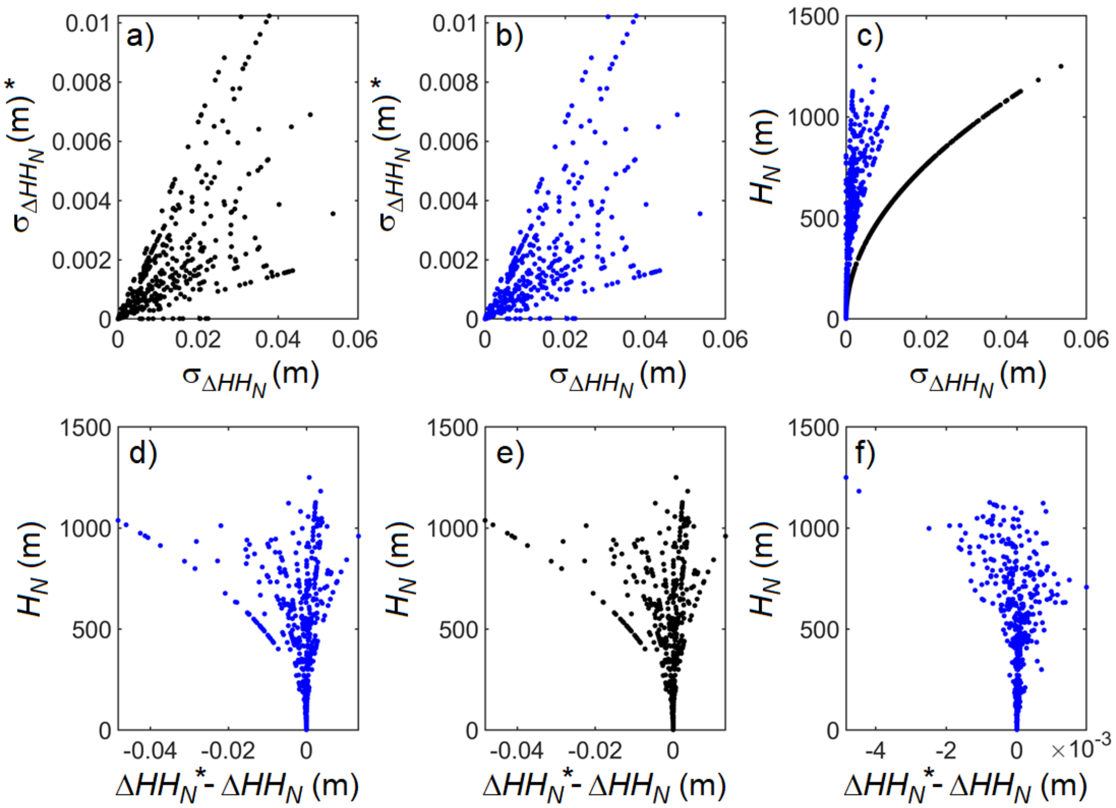

Figure 4: $\sigma_{\Delta HH_N}$ value distribution considering: a) $H_{H\,\rho(con)} - H_N$ (horizontal axis) and $H_{H\,\rho(var)} - H_N$ (vertical axis) and b) $H_{M\,\rho(con)} - H_N$ (horizontal axis) and $H_{M\,\rho(var)} - H_N$ (vertical axis). c) $\sigma_{\Delta HH_N}$ versus H_N value distribution considering $H_{M\,\rho(con)} - H_N$ (black color) and $H_{M\,\rho(var)} - H_N$ (blue color). ΔHH_N difference values versus H_N, considering d) $H_{M\,\rho(var)} - H_N$ and $H_{M\,\rho(con)} - H_N$, e) $H_{H\,\rho(var)} - H_N$ and $H_{H\,\rho(con)} - H_N$ and f) $H_{M\,\rho(var)} - H_N$ and $H_{H\,\rho(var)} - H_N$. * individualizes the H values used in estimating ΔHH_N.

From the results presented in Figures 4d, and 4e, it is possible to verify that ΔHH_N difference values are more sensitive to the ρ values and greater heights than for the Helmert and Mader method (Figure 4f) used to estimate values of H. Furthermore, analyzing Figures 4a, 4b and 4c, it is considered that the uncertainties have the same behavior for both methods, and the lowest values are presented for variable values of ρ. Also, it is important to comment that the uncertainties shown in Figure 4c are strongly influenced by the high correlation, or high covariance values, between H_N and H.

To corroborate our analyses from the results presented in Figure 4, Figure 5 shows the dispersion of ΔHH_N versus H_N, in which we observe that the largest discrepancy between the used methods occurs for greater heights.

From the achieved results (Figures 4 and 5), we may suggest that the significant differences are mainly located in regions with great heights and relief variations. This is because the amount of topographic masses above the geoid surface, associated with the heights, is used to compute the mean gravity value along the plumb line. Consequently, the greater the amount of topographic masses, the greater is the difference between $\bar{g}$ (Equations 8 to 13) and $\bar{\gamma}$ (Equations 3 and 4). Also, it is important to consider that the uncertainties estimated in this research are largely influenced by the uncertainties of normal heights (Figure 2), which are estimated by IBGE. Therefore, a change in uncertainties from a new RAAP adjustment by IBGE will likely influence the results.

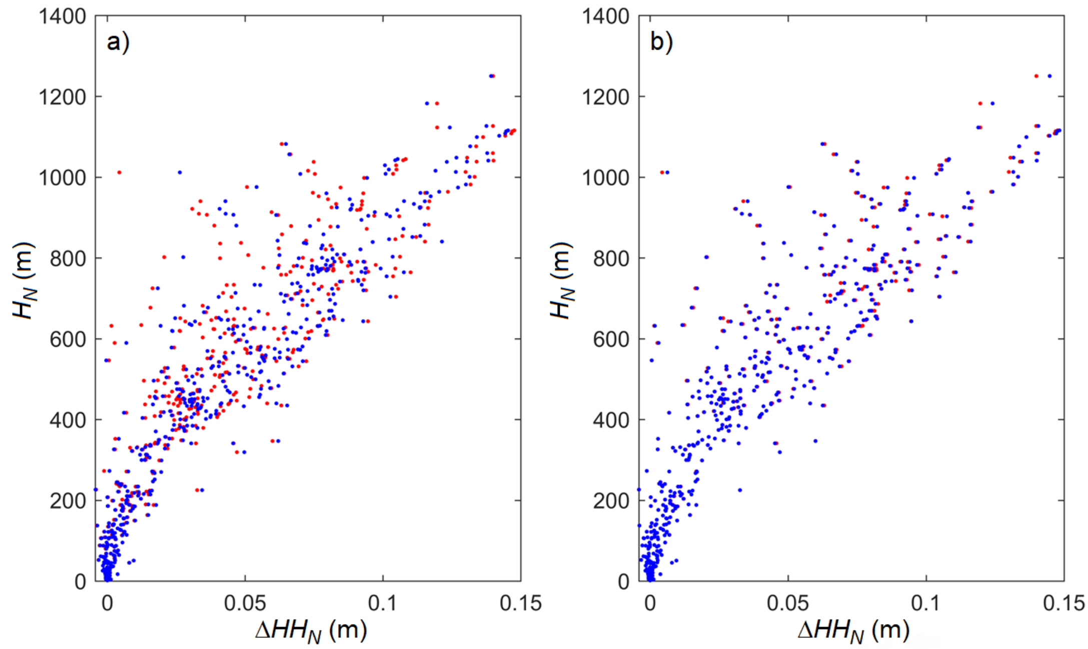

Figure 5: Dispersion of the ΔHH_N values in relation to the H_N, considering: a) $H_{M\,\rho(var)}$ (red color), $H_{M\,\rho(con)}$ (blue color) and b) $H_{M\,\rho(var)}$ (red color), $H_{H\,\rho(var)}$ (blue color).

Despite the similarity between the achieved results, we have to stress that $H_{M\,\rho(var)}$ involves a more rigorous formulation since it takes into account terrain correction terms. Therefore, in Figures 6, 7 and 8 we plot the spatial distribution of the $\Delta HH_N \pm \sigma_{\Delta HH_N}$, H and $N \pm \sigma_N$, respectively, considering the $H_N \pm \sigma_{H_N}$, $H_{M\,\rho(var)} \pm \sigma_{H_{M\,\rho(var)}}$ and $h \pm \sigma_h$ for all stations.

As the values of $\sigma_{H_{M\,\rho(var)}}$ are very close to σ_{H_N} (differences less than 1 mm), it is assumed that the spatial distribution of $\sigma_{H_{M\,\rho(var)}}$ may be represented by Figure 2.

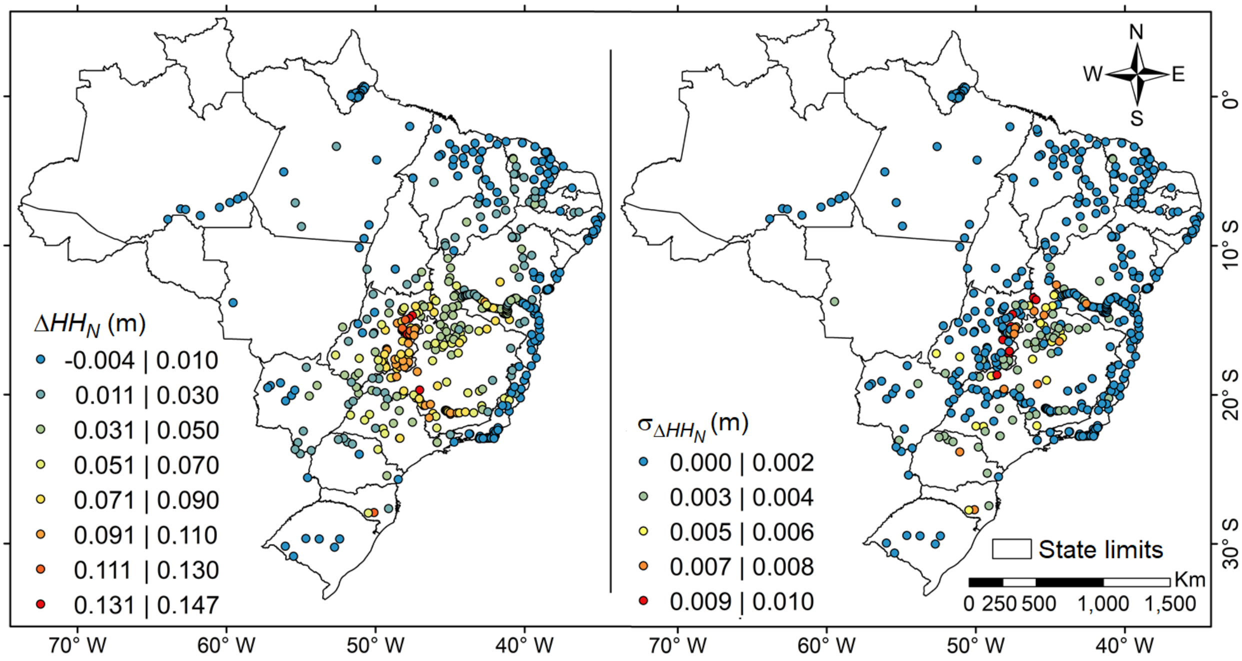

Figure 6: Spatial distribution of $\Delta HH_N \pm \sigma_{\Delta HH_N}$ computed using $H_N \pm \sigma_{H_N}$ and $H_{M\,\rho(var)} \pm \sigma_{H_{M\,\rho(var)}}$.

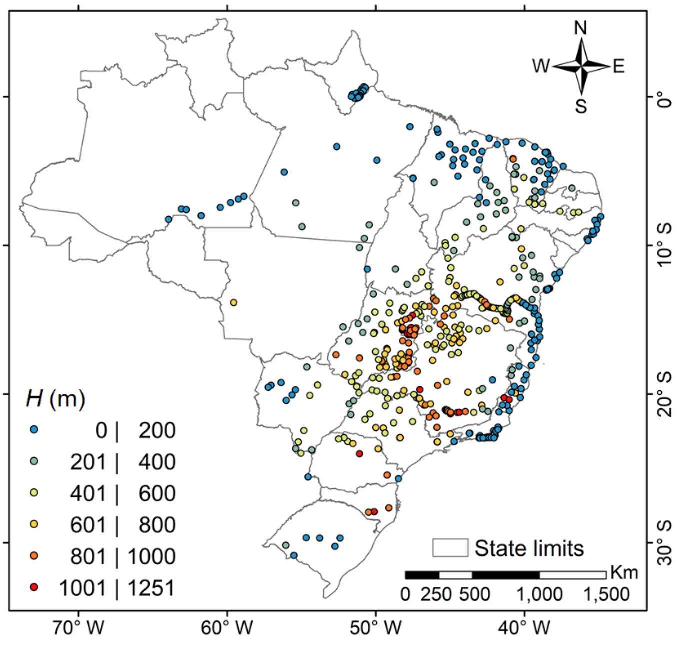

Figure 7: Spatial distribution of $H_{M\,\rho(var)}$.

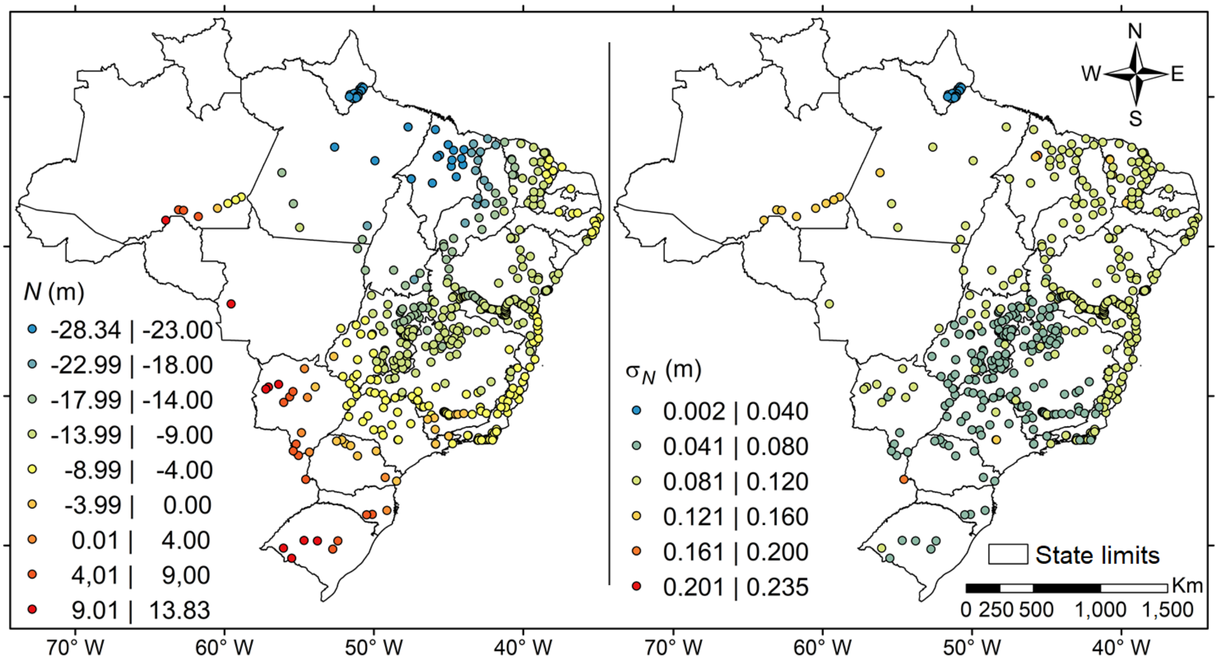

Figure 8: Spatial distribution of $N \pm \sigma_N$ computed using $h \pm \sigma_h$ and $H_{M\,\rho(var)} \pm \sigma_{H_{M\,\rho(var)}}$.

From the results presented in Figures 6, 7, 2 and 8, we observe a great influence of the normal heights uncertainties on our estimates. Normal heights uncertainties are smaller for the RAAP stations closer to the vertical datum of Imbituba and Santana, defined for the SGB. Here, it is important to mention that the Santana vertical datum is used only for stations located near or the north the Amazon River, while the Imbituba vertical datum is used for all other stations located in the Brazilian territory.

Finally, when analyzing Figures 6, which shows differences between H and H_N greater than the estimated uncertainties, it is possible to suggest that both heights are statistically different when 1σ or a 68.3% confidence level is taken into account.

5. Conclusion

In this work, we use the Helmert and Mader methods, assuming constant and variable density values, for the computation of orthometric heights. After uncertainty analysis, we calculate geoid heights for 569 stations from the High Precision Altimetric Network of Brazil for their use in the development of new geoid models derived from gravimetric and positioning data.

Due to the results presented by the differences between orthometric and normal heights, it is possible to verify that the values of orthometric heights are more sensitive to the values of density and to greater heights than the Helmert and Mader methods applied. Furthermore, we find out that the uncertainties have the same behavior for both methods, and the lowest values are presented using variable density values.

Still analyzing the differences between orthometric and normal heights, the values presented are greater than the estimated uncertainties for most used stations, and it is possible to suggest that both heights are statistically different when 1σ or a 68.3% confidence level is taken into account.

Despite the similarity between the results we find in this study, we consider that the use of the Mader method and variable density values may provide more rigor and confidence to the results. Therefore, from this premise, the orthometric and geoid heights are presented with their respective uncertainties for each station used in this research.

Finally, this research highlights the importance of considering the data uncertainties, more rigorous functional models, and variable density values for the computation of orthometric and geoid heights. This is mainly motivated by the extensive use of *GNSS* positioning and the importance of proper heights for different studies.

ACKNOWLEDGMENT

The authors acknowledge the IBGE, Medeiros et al. (2021), Sheng et al. (2019) and Farr et al. (2007) for providing the data used in this research. We thank the editors and reviewers for reading and thoughtful comments on our manuscript, and UnB (University of Brasília), DNIT (National Department of Transport Infrastructure), FAPDF (0193.001230/2016 and 00193.00001526/2021-93) and CAPES (Finance Code 001) for the technical and financial support to this research. All computation procedures were performed using routines developed in MATLAB®. Figures were created using ArcGIS® software.

The final dataset of this research is available from the following web address: https://doi.org/10.5281/zenodo.5593680.

AUTHOR´S CONTRIBUTION

Author 1 developed the methodology, investigation, formal analysis, validation and wrote the manuscript. Author 2 performed the supervision and developed the methodology, computational routines, investigation, formal analysis, validation and wrote the manuscript. Authors 3 and 4 developed the investigation, formal analysis, validation and wrote the manuscript.

REFERENCES

Albarici, F. L. Guimarães, G. N. Foroughi, I. Santos, M. Trabanco, J. L. A. 2018. Separação entre Geoide e Quase-Geoide: Análise das Diferenças Entre as Altitudes Normal-Ortométrica e Ortométrica Rigorosa [Separation Between Geoid and Quasi-Geoid: Analysis of the Diferences Between Normal-Orthometric and Rigorous Orthometric Heights]. *Anuário do Instituto de Geociências - UFRJ*, 41, pp. 71-81. https://doi.org/10.11137/2018_3_71_81

Amarante, R. R. Trabanco, J. L. 2016. Calculation of the tide correction used in gravimetry. *Revista Brasileira de Geofísica*, 34(2), pp. 193-206. http://dx.doi.org/10.22564/rbgf.v34i2.793

Bizzi L. A. Schobbenhaus, C. Vidotti, R. M., Gonçalves, J. H. 2003. *Geologia, tectônica e recursos minerais do Brasil: texto, mapas e SIG* [*Geology, tectonics and mineral resources in Brazil: text, maps and GIS*]. Serviço Geológico do Brasil - CPRM, 692 p.

Dennis, M. Featherstone, W. 2003. *Evaluation of Orthometric and Related Height Systems Using a Simulated Mountain Gravity Field*, in I N Tziavos (ed), 3rd Meeting of the International Gravity and Geoid Commission, Thessaloniki, Greece: Ziti Editions, pp. 389-394.

Drewes, H. Sánchez, L. Blitzkow, D. Freitas, S. R. C. 2002. Scientific Foundations of the SIRGAS Vertical Reference System. *Vertical Reference System - VeReS*, Springer, Berlin, 197-301. http://dx.doi.org/10.1007/978-3-662-04683-8_55

Featherstone, W. E. Dentith, M. C. 1997. A Geodetic Approach to Gravity Data Reduction for Geophysics. *Computers & Geosciences*, 23(10), 1063-1070.

Farr, T. G. Rosen, P. A. Caro, E. Crippen, R. Duren, R. Hensley, S. Kobrick, M. Paller, M. Rodriguez, E. Roth, L. Seal, D. Shaffer, S. Shimada, J. Umland, J. Werner, M. Oskin, M. Burbank, D. Alsdorf, D. 2007. The Shuttle Radar Topography Mission. *Reviews of Geophysics*, 45, RG2004. https://doi.org/10.1029/2005RG000183

Ferreira, V.G. Freitas, S. R. C. Heck, B. 2011. A Separação entre o Geoide e o Quase-Geoide: Uma Análise no Contexto Brasileiro [The Separation Between Geoid and Quasigeoid: an Analysis in the Brazilian Context]. *Revista Brasileira de Cartografia*, 63, pp.39-50.

Flury, J. Rummel, R. 2009. On the Geoid-Quasigeoid Separation in Mountain Areas. *Journal of Geodesy*, 83, pp.829-847. https://doi.org/10.1007/s00190-009-0302-9

García-Abdeslem, J. 2020. On the seawater density in gravity calculations. *Journal of Applied Geophysics*, 183, pp. 104200. https://doi.org/10.1016/j.jappgeo.2020.104200

Hayford, J. Bowie, W. 1912. *Geodesy: Effect of Topography and Isostatic Compensation upon the Intensity of Gravity*. Special Publication No. 10, U.S. Coast and Geodetic Survey.

Heiskanen, W. A. Moritz, H. 1967. *Physical Geodesy*, San Francisco: W.H. Freeman and Co.

Helmert, F. 1890. *Die Schwerkraft im Hochgebirge, insbesondere in den Tyroler Alpen*. Veröff. Königl. Preuss. Geod. Inst, 1.

Hinze, W. J. 2003. Bouguer Reduction Density, Why 2.67. *Geophysics*, 68(5), pp. 1559-1560. https://doi.org/10.1190/1.1620629

Huang, J. Vaníček, P. Pagiatakis, S. D. Brink, W. 2001. Effect of Topographical Density on Geoid in the Canadian Rocky Mountains. *Journal of Geodesy*, 74(11/12), pp. 805-815. https://doi.org/10.1007/s001900000145

Hwang, C. Hsiao, Y. S. 2003. Orthometric Corrections from Leveling, Gravity, Density and Elevation Data: A Case Study in Taiwan. *Journal of Geodesy*, 77, pp. 279-291. http://dx.doi.org/10.1007/s00190-003-0325-6

IAG - International Association of Geodesy. Resolution nº 1. Prague, July 2015. Available at: <https://iag.dgfi.tum.de/fileadmin/IAG-docs/IAG_Resolutions_2015.pdf>. [accessed: 10 December 2020].

IGN - Instituto Geográfico Nacional. 2017. Red Nivelación de la República Argentina [Leveling Network of the Argentine Republic]. Available from: <https://ramsac.ign.gob.ar/posgar07_pg_web/documentos/Informe_Red_de_Nivelacion_de_la_Republica_Argentina.pdf> [accessed: 10 December 2020].

IBGE - Instituto Brasileiro de Geografia e Estatística. 2018. Reajustamento da rede altimétrica com números geopotenciais REALT-2018 [Readjustment of the Altimetric Network with Geopotential Numbers REALT-2018]. Available from: <https://biblioteca.ibge.gov.br/visualizacao/livros/liv101594.pdf> [accessed: 10 December 2020].

Kiamehr, R. 2006. The Impact of Lateral Density Variation Model in the Determination of Precise Gravimetric Geoid in Mountainous Areas: A Case Study of Iran. *Geophysical Journal International*, 167(9), pp. 521-527. http://dx.doi.org/10.1111/j.1365-246X.2006.03143.x

Kuhn, M. 2000. Density modelling for geoid determination. International Association of Geodesy Symposia, Vol. 123. Sideris (ed.), *Gravity, Geoid, and Geodynamics 2000*, Springer - Verlag Berlin Heidelberg 2001. http://dx.doi.org/10.1007/978-3-662-04827-6_46

Li, Y. C. Sideris, M. G. 1994. Improved Gravimetric Terrain Corrections. *Geophysical Journal International*, 119, pp 740-752. https://doi.org/10.1111/j.1365-246X.1994.tb04013.x

Mader, K. 1954. *Die Orthometrische Schwerekorrektion des Präzisions-Nivellements in den Hohen Tauern* [The orthometric gravity correction for precision leveling in the Hohe Tauern]. Österreichische Zeitschrift für Vermessungswesen, Special Issue 15. https://www.ovg.at/static/vgi-sonderhefte/sonderheft1954_15_final_OCR.pdf

Marotta, G. S. 2020. Adjustment of a regional altimetric network, in Brazil, to estimate normal heights and geopotential numbers. *Boletim de Ciências Geodésicas*, 26, p.p. e2020002. https://doi.org/10.1590/s1982-21702020000100002

Marotta, G. S. Almeida, M. A. Chuerubim M. L. 2019. Análise da Influência do Valor de Densidade na Estimativa do Modelo Geoidal Local para o Distrito Federal, Brasil [Analysis of the Influence of the Density Value on the Estimation of the Local Geoid Model for the Federal District, Brazil]. *Revista Brasileira de Cartografia*, 71 (4), pp.1089-1113. https://doi.org/10.14393/rbcv71n4-49274

Martinec, Z. Vaníček, P. Mainville, A. Véronneau, M. 1995. The Effect of Lake Water on Geoidal Height. *Journal of Geodesy*, 20(3), pp. 193-203.

Medeiros, D. F. Marotta, G. S. Yokoyama, E. Franz, I. B. Fuck, R. A. 2021. Developing a lateral topographic density model for Brazil. *Journal of South American Earth Sciences*, 110, pp. 103425. https://doi.org/10.1016/j.jsames.2021.103425

Niethammer, T. 1932. *Nivellement und Schwere als Mittel zur Berechnung wahrer Meereshöhen*. Schweizerische Geodätische Kommission, Berne.

Pagiatakis, S. D. Armenakis, C. 1999. Gravimetric Geoid Modelling with GIS. *International Geoid Service Bulletin*, 8, pp. 105-112.

Pick, M. Pícha, J. Vyskočil, V. 1973. *Theory of the Earth's Gravity Field*. Elsevier, Amsterdam.

Ramsayer, K. 1953. *Die Schwerereduktion von Nivellements* [The weight reduction in leveling]. Deutsche Geodätische Kommission, Reihe A, Heft 6, München.

Ramsayer, K. 1954. Vergleich Verschiedener Schwerereduktionen Von Nivellements [Comparison of different gravity reductions for leveling]. *Zeitschrift* für *Vermessungswesen*, 79, pp. 140-150.

Rózsa, S. 2002. Local Geoid Determination Using Surface Densities. *Periodica Polytechnica Ser. Civ. Eng.*, 46 (2), pp. 205-212.

Santos, M. C. Vaníček, P. Featherstone, W. E. Kingdon, R. Ellmann, A. Martin, B. - A. Kuhn, M. Tenzer, R. 2006. The Relation Between Rigorous and Helmert's Definitions of Orthometric Heights. *Journal of Geodesy*, 80(12), p.p. 691-704. https://doi.org/10.1007/s00190-006-0086-0

Sheng, M. B. Shaw, C. Vaníček, P. Kingdon, R. W. Santos, M. Foroughi, I. 2019. Formulation and Validation of a Global Laterally Varying Topographical Density Model. *Tectonophysics*, 762, pp. 45-60. https://doi.org/10.1016/j.tecto.2019.04.005

SIRGAS – Sistema de Referência Geocéntrico para las Américas. National densifications of SIRGAS. Available from: <http://www.sirgas.org/>. [accessed: 10 December 2020].

Sánchez, J. L. C. Freitas, S. R. 2016. Estudo do Sistema Vertical de Referência do Equador no Contexto da Unificação do Datum Vertical [Study of the Ecuadorian Vertical Reference System in the Vertical Datum Unification Context]. *Boletim de Ciências Geodésicas*, 22(2), pp.248-264.

Sjöberg, L.E. 2018. On the Geoid and Orthometric Height vs. Quasigeoid and Normal Height. *Journal of Geodetic Science*, 8(1), pp.115-120. https://doi.org/10.1515/jogs-2018-0011

Sjöberg L. 2010. A Strict Formula for Geoid-to-Quasigeoid Separation. *Journal of Geodesy*, 84(11), pp. 699-702. https://doi.org/10.1007/s00190-010-0407-1

Sjöberg, L. E. 2004. The Effect on the Geoid of Lateral Density Variations. *Journal of Geodesy*, 78 (1/2), pp. 34-39. https://doi.org/10.1007/s00190-003-0363-0

Tenzer, R. Novák, P. Moore, P. Kuhn, M. Vaníček, P. 2006. Explicit Formula for the GeoidQuasigeoid Separation. *Studia Geophysica et Geodaetica*, 50, pp. 607-618. https://doi.org/10.1007/s11200-006-0038-4

Tenzer, R. Sirguey, P. Rattenbury, M. Nicolson, J. 2011. A Digital Rock Density Map of New Zealand, *Computer & Geosciences*, 37(8), pp. 1181-1191. https://doi.org/10.1016/j.cageo.2010.07.010

Torge, W. 1991. Geodesy. 2nd ed. Berlin; New York: de Gruyter.

Tziavos I. N. Featherstone, W. E. 2001. First Results of Using Digital Density Data in Gravimetric Geoid Computation in Australia. In: Sideris M.G. (eds) *Gravity, Geoid and Geodynamics 2000*. International Association of Geodesy Symposia, 123. Springer, Berlin, Heidelberg. https://doi.org/10.1007/978-3-662-04827-6_56

Tocho, C. N. Antokoletz, E. D. Piñón, D. A. 2020. Towards the Realization of the International Height Reference Frame (IHRF) in Argentina. *International Association of Geodesy Symposia*. http://dx.doi.org/10.1007/1345_2020_93

Vaníček, P. Santos, M. S. Tenzer, R. Navarro, A. H. 2003. Algunos Aspectos Sobre Alturas Ortométricas y Normales [Some Aspects About Normal and Orthometric Heights]. *Revista Cartográfica*, 76/77, pp. 79-86.